The Cryosphere Discuss., https://doi.org/10.5194/tc-2018-92
Manuscript under review for journal The Cryosphere
Discussion started: 28 May 2018

The Cryosphere Discussions
Open Access

Snow depth uncertainty and its implications on satellite derived Antarctic sea ice thickness

Daniel Price[1], Iman Soltanzadeh[2] & Wolfgang Rack[1]

[1]Gateway Antarctica, University of Canterbury, Private Bag 4800, Christchurch, New Zealand
[2]Met Service, 30 Salamanca Road, Kelburn, Wellington, 6012, New Zealand

Correspondence to: Daniel Price (daniel.price@canterbury.ac.nz)

Abstract. Knowledge of the snow depth distribution on Antarctic sea ice is poor but is critical to obtaining sea ice thickness from satellite altimetry measurements of freeboard. We examine the usefulness of various snow products to provide snow depth information over Antarctic fast ice with a focus on a novel approach using a high-resolution numerical snow accumulation model (SnowModel). We compare this model to results from ECMWF ERA-Interim precipitation, EOS Aqua AMSR-E passive microwave snow depths and *in situ* measurements at the end of the sea ice growth season. The fast ice was segmented into three areas by fastening date and the onset of snow accumulation was calibrated to these dates. SnowModel falls within 0.02 m snow water equivalent (swe) of *in situ* measurements across the entire study area, but exhibits deviations of 0.05 m swe from these measurements in the east where large topographic features appear to have caused a positive bias in snow depth. AMSR-E provides swe values half that of SnowModel for the majority of the sea ice growth season. The coarser resolution ERA-Interim, not segmented for sea ice freeze up area reveals a mean swe value 0.01 m higher than *in situ* measurements. These various snow datasets and *in situ* information are used to infer sea ice thickness in combination with CryoSat-2 (CS-2) freeboard data. CS-2 is capable of capturing the seasonal trend of sea ice freeboard growth but thickness results are highly dependent on the assumptions involved in separating snow and ice freeboard. With various assumptions about the radar penetration into the snow cover, the sea ice thickness estimates vary by up to 2 m. However, we find the best agreement between CS-2 derived and *in situ* thickness when a radar penetration of 0.05-0.10 m into the snow cover is assumed.

1 Introduction

The understanding of Antarctic sea ice has greatly improved over the last few decades, principally supported by advancements in satellite capability. Nevertheless, many knowledge gaps remain which restrict further developments. A foremost concern is inadequate data for the snow depth distribution on Antarctic sea ice (Pope et al., 2016) as the presence of snow has many important implications for the sea ice cover (Massom et al., 2001, Wu et al., 1999, Fichefet and Maqueda, 1999). The thermal conductivity of snow is almost an order of magnitude less than sea ice (Maykut and Untersteiner, 1971) and as snow accumulates, it reduces the conductive heat flux from the ocean to the atmosphere, slowing growth rates, but also leads to thickening of the ice cover through snow-ice formation (Maksym and Markus, 2008). Snow significantly increases the albedo of the sea ice cover and in the austral spring and summer snow melt drives fresh water input to the Southern Ocean (Massom et al., 2001). Crucially it is highly influential from an observational perspective given our restricted ability to combine reliable snow depth information with altimetric measurements from satellites. Sea ice thickness measurements as inferred via satellite freeboard estimates (Schwegmann et al., 2016, Kurtz and Markus, 2012, Giles et al., 2008) currently present the the best opportunity to establish yet unpublished datasets on decadal trends in Antarctic sea ice volume. Dedicated basin-scale snow depth assessments have been completed (Markus and Cavalieri, 2006) but continual improvements in our monitoring ability are key to support the current ESA satellite altimeter missions, CryoSat-2 (CS-2) and Sentinel-3 and NASA's planned ICESat-2 expected to be operational in late 2018. Without improved snow depth measurements, it is impossible to discern meaningful trends in Antarctic sea ice thickness. Errors are introduced to thickness estimates via the snow cover for two principal reasons:

1. Snow depth information is inaccurate/not available and therefore the ratio of ice and snow above the waterline is poorly quantified or unknown.
2. The presence of snow influences incident radar energy which manifests itself in the radar waveform. If the retracking procedure does not accurately account for this, the retracked surface, assumed to be freeboard, will be incorrect.

Arctic sea ice has been investigated in more detail and over a longer period than the Antarctic permitting the compilation of snowfall climatologies (Warren et al., 1999). These datasets in combination with satellite altimetry, and suitable airborne investigations have permitted the completion of pan-Arctic thickness assessments (Kurtz et al., 2014, Laxon et al., 2013, Kwok and Cunningham, 2008). The research community lacks this information in the Southern Ocean; to date AMSR-E passive microwave data have been used to establish snow depth. The algorithm's accuracy is decreased by rough sea ice and deep and complex snow (Kern and Ozsoy-Çiçek, 2016, Kern et al., 2011, Worby et al., 2008b, Stroeve et al., 2006), both typical characteristics of the Antarctic sea ice cover. Some investigators have assumed zero ice freeboard (Kurtz and Markus, 2012), that is, the snow loading forces the ice surface to the waterline, negating the need for snow depth data. Thickness estimates using this approach are likely biased low and although this simplification provides valuable insights, it does not provide sea ice thickness at the desired accuracy. More work is required to adequately map the complex regional characteristics of the snow cover. This work is motivated by the necessity for a comprehensive understanding of the usefulness of snow products in the Southern Ocean, and the need to investigate new avenues for producing snow depth products over Antarctic sea ice. Here we make use of a detailed *in situ* dataset to assess satellite and modelling approaches to construct snow depth over the 2011 sea ice growth season. With a high-resolution snow accumulation model called SnowModel (Liston and Elder, 2006a) and the use of synthetic aperture radar imagery we are able to establish sea ice fast-day-zero and accumulate snow from those dates for three areas of fast ice in McMurdo Sound in the south-western Ross Sea. The high-resolution model results are compared to snow depths acquired via two independent datasets, another model of lower resolution, ERA-Interim and passive microwave satellite data from AMSR-E. With these different snow depth datasets we infer sea ice thickness via freeboard measurements from CryoSat-2 and assess uncertainty using *in situ* information.

The Cryosphere Discuss., https://doi.org/10.5194/tc-2018-92
Manuscript under review for journal The Cryosphere
Discussion started: 28 May 2018

2 Study area, field and satellite data

2.1 McMurdo Sound and field data

A detailed *in situ* sea ice measurement campaign was carried out in November 2011 on the fast ice in McMurdo Sound (Fig. 1). This involved sea ice thickness, freeboard and snow depth/snow density measurements at 39 sites. Mean snow depths for each *in situ* site represent 60 individual snow depth measurements in a cross-profile at each site. A full overview of the measurement procedure is provided in Price et al. (2014).

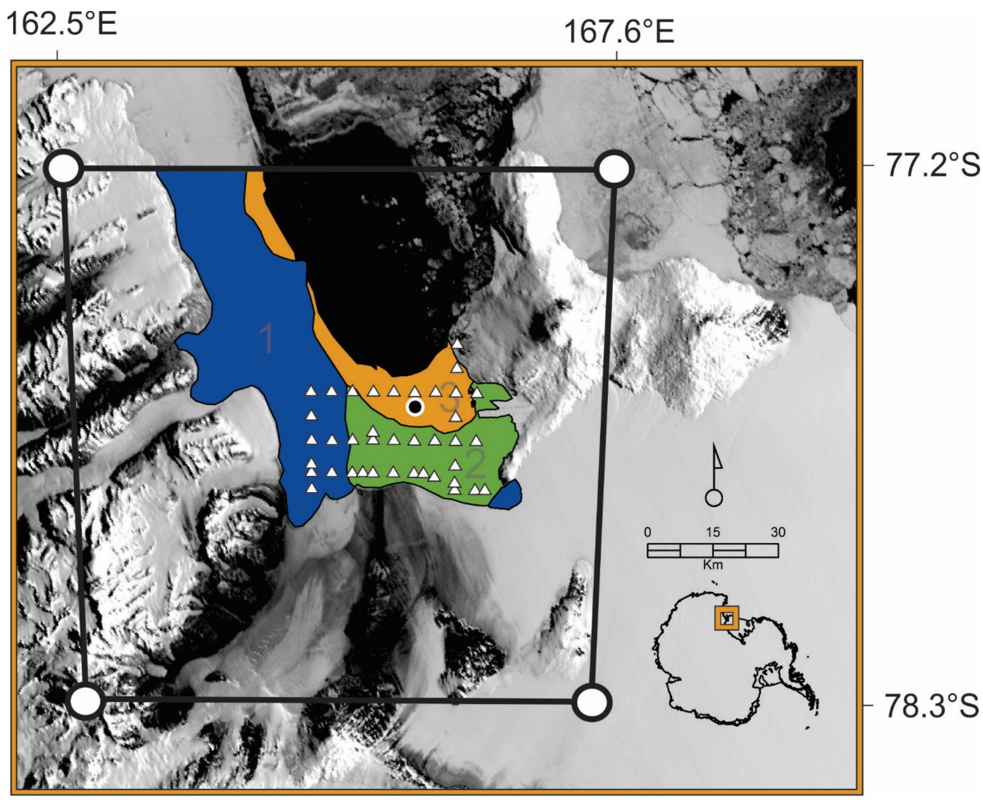

Figure 1. McMurdo Sound study area with each fast-day-zero area as identified by Envisat radar imagery: Area 1 – 01/04/2011 (Blue), Area 2 – 29/04/2011 (Green), Area 3 – 01/06/2011 (Orange) and SnowModel domain bounded by black box. Freeze-up areas are superimposed on a MODIS image acquired on 15 November at the time of maximum fast ice extent in 2011. The locations of 39 measurement sites used to produce the *in situ* snow statistics are shown as white triangles. The position of the virtual weather station created to retrieve ERA-Interim atmospheric reanalysis products is identified by the black circle.

2.2 Envisat

The timing of the sea ice fastening must be known (fast-day-zero) in order to provide a point at which snow can begin to accumulate. We use a string of Envisat ASAR images acquired during the freeze up season to establish this date and in what pattern the ice fastened. We identify three areas that froze independently of one another. Large areas of fast ice were established by 1 April (Area 1 – Fig. 1), by the end of April, a second area of fast ice had formed along the southern extremity of the sound (Area 2 – Fig. 1), and by the beginning of June, a third area had fastened (Area 3 –Fig. 1). These three areas persisted for the winter and when combined made up the fast ice area present in late November, when *in situ* measurements were made.

2.3 AMSR-E

The EOS Aqua Advanced Microwave Scanning Radiometer (AMSR-E) was operational from December 2002 until 4 October 2011. Snow depth is averaged over an approximate area of 25 x 25 km^2, gridded to a 12.5 x 12.5 km^2 polar stereographic projection and reported as a 5-day running mean, that mean inclusive of that day and the prior 4 days. Multiple flags are used to identify poor data retrievals, of relevance to this study are data flagged as 130 where ice concentrations are lower than 20%. No data are provided in these cells. Gridded snow depth values are calculated using the spectral gradient ratio of the 18.7 and 37 GHz vertical polarisation channels. Scattering efficiency is greater at 37 GHz than at 19 GHz, and as scattering universally increases across both frequencies with increasing snow depth, the gradient ratio between the channels becomes increasingly negative (Comiso et al., 2003, Markus and Cavalieri, 1998). Snow depth retrievals are restricted to dry snow only and to a depth of less than 50 cm. Variable snow properties including snow grain size, snow density and liquid water content influence microwave emissivity from the sea ice surface and the algorithm is reported to have a precision of 5 cm (Comiso et al., 2003) . Given the extreme southern latitude of the study area, snow conditions throughout this study were very dry, supported by snow pit analysis on the sea ice in November with no wet snow or lensing observed. AMSR-E cells are included in the analysis if over 50% of the cell lies within the fast ice mask, and segmented into each freeze up area by that same criteria. 22 AMSR-E cells are used in the analysis and due to the instrument failure in early October 2011, data for the last two months of this investigation are unavailable.

2.4 CryoSat-2

CS-2 is a *Ku*-band (center frequency 13.6 GHz) radar altimeter launched in 2010. In section 6, to assess the accuracy of the evaluated snow products, we infer sea ice thickness from CS-2 freeboard measurements. The ESA L2 baseline C SIN mode (SIR_SIN_L2) data set is used to estimate freeboard; the processing closely follows that described in Price et al (2015), but to reduce noise, two modifications are made to achieve more detailed scrutiny of the CS-2 height retrievals. The first is a more stringent measure for the inclusion of off-nadir elevation retrievals, the threshold is halved from ± 750m to ± 375 m; data located at greater distances from nadir are discarded. The second is the rejection of freeboard measurements of less than -0.24 m and greater than 0.74 m. Following Schwegmann et al (2016) the ± 0.24 m accounts for speckle range noise in the CS-2 data and the + 0.5 m threshold additionally incorporates an expected maximum sea ice freeboard of 0.5 m for fast ice in McMurdo Sound in 2011. Each CS-2 freeboard measurement (*Fb*) is cross-referenced to the fast-day-zero mask and assigned a snow depth (*Ts*) value from the described snow products. Sea ice thickness (*Ti*) is then derived using varying freeboards as there is currently no consensus on what this surface represents over sea ice, the air-snow interface, the snow-ice interface or an undefined interface between the two. Laboratory experiments (Beaven et al., 1995) and comparisons of other radar altimeter systems with *in situ* measurements (Laxon et al., 2003) suggest the snow-ice interface

The Cryosphere Discuss., https://doi.org/10.5194/tc-2018-92
Manuscript under review for journal The Cryosphere
Discussion started: 28 May 2018

is detected. It is clear the presence of snow influences the CS-2 height retrieval but precisely how is dependent on its depth (Kwok, 2014) and its dielectric properties (Hallikainen et al., 1986). The mean depth of the dominant backscattering surface measured using a surface based *Ku*-band radar over snow covered Antarctic sea ice was around 50% of the mean measured snow depth, and the snow-ice interface only dominated when morphological features or flooding were absent (Willatt et al., 2010). Beyond Wingham et al. (2006) who indicate the snow-ice interface is assumed, no information is available about the assumptions for the ESA retracking procedure, only that for diffuse echoes in SAR processing for baseline C a new retracker was implemented (Bouffard, 2015). It is unclear what the original retracking assumptions are for any retrieval mode and if any changes were made to SIN mode for baseline C. A prior study of CS-2 waveform behaviour over the same study area found ESA L2 freeboard to be located between the air-snow and snow-ice interface (Price et al., 2015). Given this uncertainty we derive sea ice thickness for a range of possibilities; Equation 1 assumes that the snow surface is detected, equation 2 that the sea ice surface is detected and equation 3 that an arbitrary surface at a given penetration depth (*Pd*) into the snow pack is detected;

$$T_i = \frac{\rho_w}{\rho_w - \rho_i} Fb - \frac{\rho_w - \rho_s}{\rho_w - \rho_i} T_s \tag{1}$$

$$T_i = \frac{\rho_w}{\rho_w - \rho_i} Fb + \frac{\rho_s}{\rho_w - \rho_i} T_s \tag{2}$$

$$T_i = \frac{\rho_w}{\rho_w - \rho_i} Fb - \frac{\rho_w - \rho_s}{\rho_w - \rho_i} T_s + \frac{\rho_w}{\rho_w - \rho_i} Pd \tag{3}$$

where ρw (1027 kgm^{-1}), ρi (925 kgm^{-1}) and ρs (385 kgm^{-1}) are the densities of water, sea ice and snow respectively as informed by *in situ* investigations. When required, for *Fb* and *Pd* reduction of the speed of the radar wave through the snow pack is corrected following the procedure described in Kurtz et al (2014).

3 Atmospheric models for snow accumulation

3.1 High resolution model

SnowModel is a numerical modelling system with four main components: (1) MicroMet, a quasi-physically-based, high-resolution meteorological distribution model (Liston and Elder, 2006b) (2) Enbal, a surface energy balance and snowmelt model (Liston et al., 1999) (3) SnowTran-3D, a wind driven snow redistribution routine (Liston et al., 2007, Liston and Sturm, 1998) and (4) SnowPack, a multilayer snow depth and water-equivalent model (Liston and Sturm, 1998). The main objective of MicroMet is to provide seamless atmospheric forcing data, both temporally and spatially to the other SnowModel components. MicroMet is capable of downscaling the fundamental atmospheric forcing such as air temperature, relative humidity, wind speed, wind direction, incoming solar radiation, incoming longwave radiation, surface pressure, and precipitation. Other SnowModel submodels simulate surface energy balance, and moisture exchanges including snow melt, snow redistribution and sublimation. SnowModel also incorporates multilayer heat-and mass-transfer processes within the snow (e.g. snow density evolution).

SnowModel is capable of initializing with both *in situ* and gridded model data and has been evaluated in many geographical locations including Greenland and Antarctica (Liston and Hiemstra, 2011; Liston and Hiemstra, 2008; Liston and Winther, 2005; Mernild et al., 2006).

SnowModel requires topography, land cover and various atmospheric forcing. The minimum meteorological requirements of the model are near-surface air temperature, precipitation, relative humidity, wind speed and direction data from Atmospheric Weather Stations (AWS) and/or gridded numerical models. Determining the influence of wind and other atmospheric forcing on snow distribution in a complex terrain requires the use of numerical atmospheric models. Many studies have demonstrated that high-resolution models are vital for simulating topographic and land-use impacts on wind, hydraulic jump and associated turbulence (Olafsson and Agustsson, 2009; Agustsson and Olafsson, 2007). For this research, hourly atmospheric forcing were generated by version 3.5 of the polar-optimized version of the Advanced Research Weather Research and Forecasting Model (WRF-ARW; Skamarock et al., 2008) known as Polar WRF (Bromwich et al., 2009) or PWRF (http://polarmet.osu.edu/PWRF) at 3 km horizontal resolution.

The WRF-ARW (hereafter, WRF) is a state-of-the-art model that is equipped with a fully compressible, Eulerian and nonhydrostatic dynamic core. This model uses Arakawa C-grid staggering in the horizontal and utilises a mass terrain-following coordinate vertically. Several physical parameterization schemes are available in WRF, and some of those used for this work are described below. The WRF single-moment 6-class microphysics scheme (WSM6; (Hong and Lim, 2006)) is a cloud microphysics scheme, which includes various water phases including graupel. This likely improves precipitation and cloud related predictions at higher spatial resolution. For radiation, the rapid radiative transfer model (RRTM;(Mlawer et al., 1997)) and the empirically based Dudhia short-wave radiation scheme (Dudhia, 1989) are used as the long and short wave radiation schemes, respectively. The Mellor–Yamada–Nakanishi–Niino (MYNN; Nakanishi and Niino, 2006, Nakanishi and Niino, 2004, Nakanishi, 2001) level-2.5 scheme is used to take into account subgrid-scale turbulent fluxes.

The Noah LSM (Chen and Dudhia, 2001) with four soil layers, which is able to handle sea-ice and polar conditions through modifications described below was chosen as the land surface model. Generally, mesoscale numerical models including WRF have simple representations for sea ice thickness and snow depth on sea ice. This shortcoming leads to an outstanding error in the simulation of the snow and mass balance in the polar regions. To address this issue, PWRF improved the representation of heat fluxes through snow and ice in the Noah LSM. Further, this version of PWRF modified sea ice and snow albedos and made it accessible to define spatially varying sea ice thickness and snow depth on sea ice [for further detailed information about PWRF see (Hines et al., 2015)].

The models, PWRF and SnowModel are coupled in an off-line manner. This means that the PWRF model ran for the entire study period first, then SnowModel initiated based on the PWRF simulated atmospheric forcing and there is no feedback from SnowModel to the atmospheric model. In order to increase the spatial resolution of the PWRF outputs, before ingesting the atmospheric forcing to the SnowModel, PWRF gridded data are interpolated to a new grid, and then corrected physically according to topography using the MicroMet submodel. The spatial resolution of SnowModel is 200 m and its output is segmented into sea ice fastening areas as indicated by the Envisat imagery (Fig. 1). These are reported as hourly means beginning at 00:00 1st April 2011 and ending at 00:00 1st December 2011. To the authors knowledge, and at the time of writing this is only the second application of SnowModel in a sea ice environment. Liston et al. (2018) applied SnowModel with an additional component that accounted for snowdrifts and snow dunes, at very high spatial resolution with positive results.

3.2 Low resolution model

ERA-Interim is a global atmospheric reanalysis product on a 0.75° x 0.75° grid available from 1 January 1989 (Dee et al., 2011). Precipitation data (mm water equivalent) are available at three hourly intervals and are converted to snow depth when required using the average snow density of 385 kgm^{-3} measured *in situ* in 2011. Data are retrieved from ERA-Interim at 77.7°S 165.8°E (Fig. 1) and accumulated through the assessment period. ERA-Interim data does not account for snow transport and does not have a high enough resolution to segregate snow accumulation by freeze up date. Therefore, the reported ERA-Interim data are daily averages for the entire study area.

4 Snow product evaluation

When the three snow products are compared to one another or to *in situ* measurements, all snow depths are reduced to snow water equivalent (swe) via their respective densities to remove any bias associated with varying density between snow datasets. SnowModel provides a swe output via a time varying snow density during the model run, AMSR-E snow depths are reduced to swe using average *in situ* measured snow density in November, and ERA-Interim precipitation is provided as swe in its original format. The SnowModel evaluation is split into two parts, firstly, an accumulation time-series is presented for SnowModel and AMSR-E segmented by fast-day-zero for areas 1 to 3 along with ERA-Interim for the entire study area (Fig. 2). Secondly, selected SnowModel grid cells are directly compared to spatially coincident *in situ* measurement sites in November (Fig. 3). The model swe value is the mean at each site between 25 November and 1 December the period over which *in situ* measurements were made.

SnowModel clearly presents two very different snow accumulation patterns, one in the west covering area 1 and one in the east covering areas 2 and 3. Mean swe values in area 1 reach a maximum of 0.02 m during the 8-month study period while in areas 2 and 3 they are in excess of 0.10 m. This is in good agreement with *in situ* measurements and general observations during fieldwork in November 2011, which recorded an increasing gradient in snow depth from west to east. Although the model captures the snow distribution on the fast ice, when each freeze-up area is directly compared to *in situ* means for those areas, swe is underestimated in area 1 (0.02 m < *in situ*), slightly overestimated in area 3 (0.01 m > *in situ*) and substantially overestimated in area 2 (0.05 m > *in situ*). Only modelled swe in area 3 falls within the standard deviation of the *in situ* mean. In the east, snow depth increases are noted in mid-May, mid-June, early-July, early and mid-August and late-September. The snow depth evolution in the west of the Sound over area 1 follows a separate pattern with negligible increases in mid/late April, mid-May, mid-July, late-September and early-November. When directly compared to *in situ* data (Fig. 3) SnowModel overestimates swe snow depth in the study area and therefore the model has better agreement with *in situ* maximum values (r^2 = 0.56) than with the mean (r^2 = 0.53) or minimum (r^2 = 0.30) values (Fig. 3).

AMSR-E snow depths tend to follow a similar pattern over time in all freeze-up areas. For areas 2 and 3, May through June, AMSR-E and SnowModel produce similar swe values, agreeing within 0.02 m. As the growth season progresses AMSR-E remains significantly lower than SnowModel swe, by up to 0.10 m. swe values are also higher in area 2 than 3 in agreement with SnowModel. However, in area 1 swe vales are four times larger than SnowModel. The longitudinal swe gradient indicated by SnowModel and supported by *in situ* data is opposite when measured using AMSR-E. As the AMSR-E instrument failed in early October, we are unable to validate it with *in situ* measurements. ERA-Interim swe for the entire study area steadily increases after the first-third of April and falls within +0.01 m of the mean of all *in situ* measurements made in November.

The Cryosphere Discuss., https://doi.org/10.5194/tc-2018-92
Manuscript under review for journal The Cryosphere
Discussion started: 28 May 2018

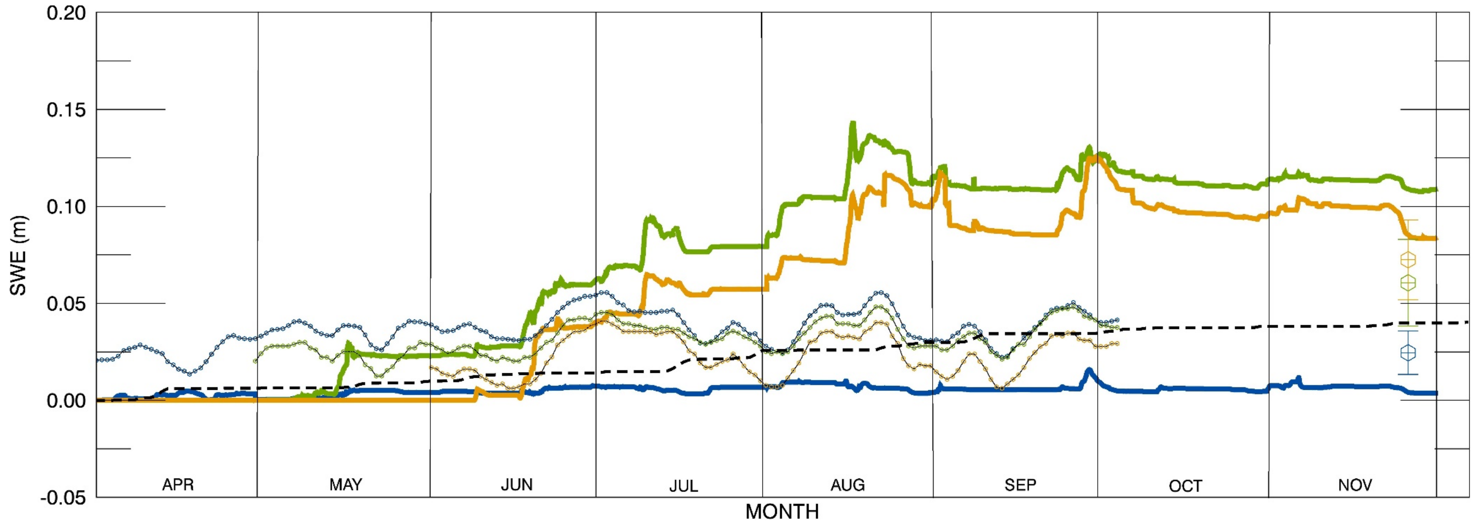

Figure 2. SnowModel (solid lines) hourly accumulation and AMSR-E daily snow depth (solid lines with circles) converted to snow water equivalent (swe) for freeze-up areas 1 (blue), 2 (green) and 3 (orange) plotted with ERA-Interim swe (hashed black line) for the entire study area. The mean *in situ* swe and standard deviations for each area are displayed as circles at the end of November and colour coded to their respective freeze-up areas.

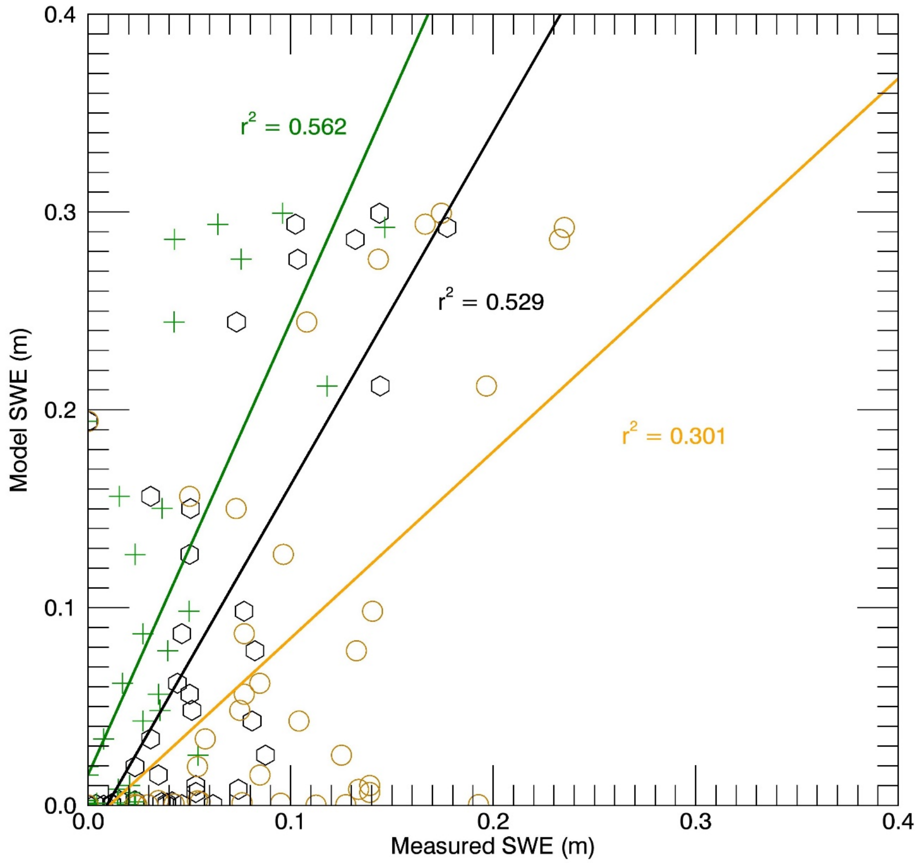

Figure 3. Mean (black), maximum (green) and minimum (orange) *in situ* measured snow water equivalent (swe) for each site against mean SnowModel swe at each coincident model cell for the *in situ* measurement period.

5 Sea ice thickness

In this section, we review the usefulness of the snow products by using them as inputs to equations 1-3 and infer sea ice thickness in McMurdo Sound through the growth season. Snow depths for each CS-2 freeboard measurement are retrieved from SnowModel directly, while ERA-Interim swe is converted to snow depth using the mean *in situ* measured density and AMSR-E provides snow depth as default. Sea ice thickness inferred from altimetry in McMurdo Sound will be influenced by the buoyant sub-ice platelet layer (Price et al., 2014). The freeboard measurement used to infer thickness is representative of the solid sea ice and the layer of sub-ice platelets attached below. Therefore, comparisons to *in situ* thickness referenced in this work actually refer to the 'mass-equivalent thickness', that is, the resultant thickness taking account of both the solid sea ice and the sub-ice platelet layer (sub-ice platelet layer multiplied by the solid fraction).

From equations 1-3, sea ice thickness is highly sensitive to the snow-ice ratio for the measured freeboard. This results in a large range in sea ice thickness for all snow products through the growth season (Fig. 4). Using modelled snow depths sea ice thickness can vary by over 2 m from assuming the air-snow interface or snow-ice interface is measured. The AMSR-E derived thickness trend is not comparable to the model output trends as the last two months are missing. However, it is useful to highlight the importance of the snow-ice freeboard ratio. AMSR-E snow depths are high in comparison to the models from the beginning of the growth season and they remain relatively stable. Because of this, the ratio of ice to snow above the waterline remains similar. The other modelled snow datasets gradually increase and snow makes up an ever increasing proportion of the freeboard. If the air-snow interface is taken to represent freeboard then the trend in sea ice thickness through the growth season is negative for the SnowModel and ERA-Interim derived thicknesses. The trend is more negative for the SnowModel estimate simply because the snow loading is greater. Thickness estimates with both modelled snow inputs give unrealistic trends, with end of season thicknesses comparable to those at the beginning of the growth season. If the snow-ice interface is assumed to represent freeboard, thickness trends are too positive. The mean CS-2 thickness values for November are 2.62 m and 2.77 m for SnowModel and ERA-Interim respectively compared to an *in situ* thickness of 2.4 m. The trends most representative of the *in situ* measurements and the known growth rate are those that assume a given *Pd* into the snow cover. For thicknesses derived using SnowModel to match *in situ* thickness a large *Pd* of 0.5 m is required given the higher snow depth values, while for ERA-Interim *Pd* values of 0.1 to 0.15 m place CS-2 thickness estimates around *in situ* thickness.

To assess this *Pd* uncertainty under more constrained conditions with regard to snow depth, we use interpolated *in situ* measurements for snow depth as input to the sea ice thickness calculation. We reduce the CS-2 measurements used in this comparison to the same area bounded by situ measurements. The total range in estimated thickness using interpolated *in situ* snow depth between equations 1 and 2 is 1.7 m. For *Pd* values 0.02 m through 0.20 m the best agreement between *in situ* thickness and CS-2 derived thickness is found between 0.05 and 0.10 m (Fig. 5), the CS-2 thickness only 0.02 m thicker than *in situ* thickness for this particular dataset when *Pd* = 0.07 m. The range in SnowModel derived thickness between equations 1 and 2 is nearly 4 m while the range when using the ERA-Interim data set is almost half that of SnowModel, showing good agreement with the *in situ* dataset (Fig. 5).

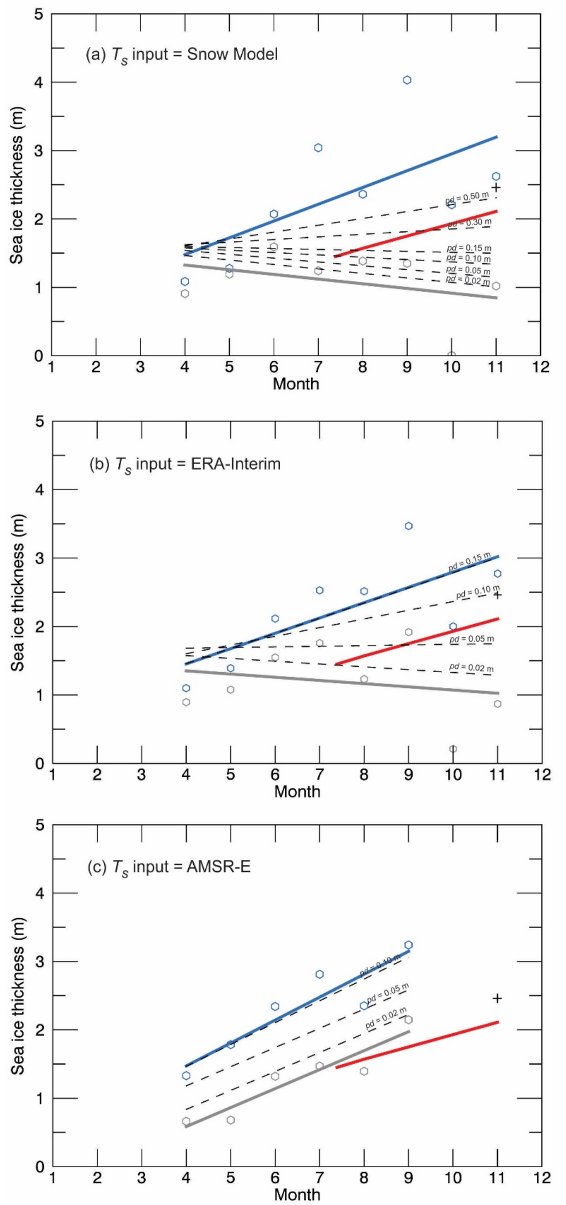

Figure 4. Sea ice thickness trends derived by CS-2 freeboard measurements with snow data provided by (a) SnowModel, (b) ERA-Interim and (c) AMSR-E. Grey dots and linear fit are sea ice thickness calculated using equation 1, blue dots and linear fit using equation 2 and dotted black lines equation 3 with varying penetration factors (*Pd*). The red line shows sea ice thickness from *in situ* measurements in July and November assuming a constant growth rate. The black plus sign is the mean 'mass-equivalent thickness' from all *in situ* measurements in November. This is slightly thicker than the end of season thickness indicated by the red line given it takes account of the influence of the sub-ice platelet too.

The Cryosphere Discuss., https://doi.org/10.5194/tc-2018-92
Manuscript under review for journal The Cryosphere
Discussion started: 28 May 2018

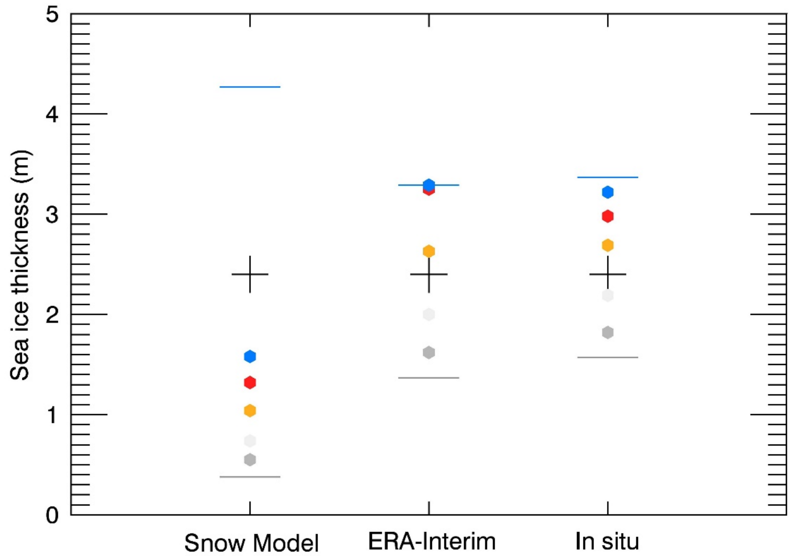

Figure 5. The range in CS-2 derived sea ice thickness in November using snow inputs from SnowModel and ERA-Interim compared to snow input from *in situ* interpolated snow depths. Thickness derived from equations 1 and 2 are shown with the grey and blue lines respectively and for equation 3 the dots are colour coded for different penetration depths (*Pd*); dark grey = 0.02 m, light grey = 0.05 m, orange = 0.10 m, red = 0.15 m and blue = 0.20 m. Black plus signs show *in situ* 'mass-equivalent thickness'. This comparison is produced from all CS-2 data height retrievals available over the *in situ* measurement area in November $n = 279$.

6 Discussion

In this section, the performance of the snow depth retrieval methods is evaluated, and we briefly discuss their future applicability to larger Antarctic sea ice areas.

Any method attempting to accumulate snow on sea ice requires the establishment of a starting date at which a sea ice surface is present. This approach used Envisat ASAR imagery and motion between scenes to identify when the sea ice fastened. Freezing may have started prior to the fastening-date but the authors are unaware of any other method to monitor freeze-up at the required spatial resolution. Sea ice could have begun to form slightly before this date which would result in an improvement in SnowModel's performance in Area 1, but increased separation between *in situ* validation and SnowModel in Areas 2 and 3. In larger open water areas, passive microwave sea ice concentration information could be used to establish the freeze up date. Detail would be lost via this method given the high (200 m) resolution of SnowModel against the coarser resolution passive microwave data.

Modelled snow depths have been evaluated in a previous work over Antarctic sea ice (Maksym and Markus, 2008), but the study produced only precipitation data while this assessment takes the next step by using a model that accounts for surface transportation, a significant redistribution mechanism in the Antarctic. Leonard and Maksym (2011) report that over half of precipitation over the Southern Ocean could be lost to leads and the application of any model to construct snow depth on sea ice in open sea areas will need to account for this. In coastal regions, local topography will also play a key role, such is the case in McMurdo Sound where Ross Island acts to encourage snow accumulation on the eastern portion of the sea ice cover. This was well replicated in SnowModel although the general overestimation of snow was driven by unrealistic values in this area, the model likely accumulating too much snow due to this topographic barrier. Smaller scale snow features such as snow drifts and snow dunes should also be accounted for in future work, as applied in a recent study by Liston et al. (2018). These meter-scale features will be important to capture, especially to support compatibility with smaller satellite altimeter footprints (e.g. ICESat-2). This work used fast ice to reduce the uncertainty associated with pack ice and use available *in situ* data to validate the snow products. To build on this approach, and make its application valuable in the Southern Ocean sea ice motion within the SnowModel domain must be incorporated.

We find ERA-Interim mean swe to be only 0.01 m lower than mean *in situ* swe in McMurdo Sound. This is a very encouraging result but we caution this result is only representative of a single year in a small area, certainly not representative of data void, open ocean regions. The performance of ECMWF reanalysis products over the satellite period is good when compared to Antarctic coastal stations (Bromwich and Fogt, 2004), but there is limited data available to assess the accuracy of these data over Antarctic sea ice. ERA-Interim ranked best among five assessed models for its depiction of interannual variability and overall change in precipitation, evaporation and total precipitable water over the Southern Ocean (Nicolas and Bromwich, 2011). Maksym & Markus (2008) used ERA-40 reanalysis for a snow assessment of the Antarctic sea ice pack but had difficulties in evaluating its accuracy. The improved reanalysis product ERA-5 has over twice the spatial resolution of ERA-Interim and given the promising results here, it should be considered for evaluation as a snow product on sea ice. The principal issue to overcome will be that reanalysis data lack any redistribution mechanism (including snow loss to leads) but parameterisations for this could be built from wind vectors provided by the same reanalysis data.

Fast ice permitted the assessment of an undisturbed sea ice area using AMSR-E. In general, when compared to SnowModel, AMSR-E underestimates snow depth in Areas 2 and 3 (eastern Sound) and overestimates snow depth in Area 1 (western Sound). Of most interest is that the clear longitudinal gradient in snow depth as indicated by SnowModel and measured *in situ* is the opposite in the AMSR-E dataset. Worby et al. (2008b) report that AMSR-E snow depths were significantly lower than *in situ* measurements on sea ice in the East Antarctic and that sea ice roughness is a major source of error using passive microwave retrieval techniques. However, they also conclude that when compared to basin-wide observations from ASPECT large differences of up to +0.20 m in the Weddell Sea and +0.05-0.10 m in the Ross Sea were noted in the AMSR-E snow depths. It is postulated that *in situ* observations underestimated true mean snow thickness as surveys were limited to level ice areas typically presenting thinner snow covers. More work is required to validate passive microwave snow depth estimates over Antarctic sea ice. No detailed sea ice surface condition survey was completed for this investigation, however from visual observations sea ice had clearly been subjected to dynamics in the west, whereas ice was very level in the east. It is possible that snow depth was underrepresented here by *in situ* measurements and that rougher sea ice in the west affected the AMSR-E retrieval algorithm. Because of the failure of the instrument, we are unable to compare AMSR-E snow depth directly to *in situ* measurements.

CS-2 has difficulty estimating freeboard over thin ice areas (Price et al., 2015, Ricker et al., 2014, Wingham et al., 2006). Here, at the beginning of the growth season CS-2 generally overestimates thickness with mean April values for SnowModel and ERA-Interim around 1 m (with the exception of AMSR-E assuming the air-snow interface is measured Ti = 0.66 m). Other investigations indicate sea ice thickness in McMurdo Sound in April is between 0.5-0.8 m (Frazer et al., under review, Gough et al., 2012, Purdie et al., 2006) . This represents a large obstacle to overcome for the application of CS-2 in the Southern Ocean as the mean thickness of Antarctic sea ice is only 0.87 m as reported from ship-based observations (Worby et al., 2008a). This supports the need for multisensor analysis, perhaps using methods already employed in the Arctic (Ricker et al., 2017, Kaleschke et al., 2012, Kwok et al., 1995). As discussed in section 2.4 assumptions must be made about what surface the freeboard measurement represents. In general, using the two modelled snow products (with trends from AMSR-E incomplete), the thicknesses derived assuming the air-snow interface is detected as freeboard are too thin and those assuming the snow-ice interface too thick. Using interpolated *in situ* measured snow depth as the snow thickness input to the thickness calculation minimises the error. With this, we find CS-2 thickness to correlate best with *in situ* thickness if *Pd* values are between 0.05-0.10 m.

The mean radar freeboard in November (not corrected for radar wave speed in the snowpack) is 0.18 m. *In situ* ice freeboard was 0.22 m and *in situ* snow freeboard was measured as 0.33 m. When corrected for radar wave speed CS-2 freeboard varies between 0.18-0.21 m (0.19-0.22 m) for SnowModel (ERA-Interim) through the full range of *Pd* assumptions (i.e. *Pd* = 0.02 m-ice freeboard detected). This result is supportive of penetration into the snowpack but it should be cautioned that this result is dependent on the established sea surface height. If the established sea surface height here has been biased high, the freeboard measurements would actually be more representative of the snow freeboard. Freeboard errors from automated sea surface height identification were in the order of 0.05 m when compared to supervised procedures in the study area (Price et al., 2015). To eliminate this uncertainty throughout the study period the sea surface would need to be manually identified for each individual CS-2 track. This is not practical for basin-scale assessments and confidence needs to be built in the sea surface height identification algorithm. The modification of the sea surface height will apply a systematic increase or decrease in freeboard making each thickness from each assumption thicker or thinner. The freeboard measurements exhibit an unexpected decrease in October and November and it is impossible to discern whether this is forced by a sea surface height that is too high or a change in the sea ice surface conditions that causes a decrease in the freeboard measurement, an additional uncertainty. It is highly plausible and in fact likely that *Pd* varies through the growth season as the snow depth and dielectric properties change. More detailed *in situ* investigations are required before a seasonally varying *Pd* can be applied. Our analysis has not taken into account a range of sea ice density assumptions but we have confidence in the value used from previous work (Price et al., 2014).

7 Conclusions

This work has evaluated the ability of three independent techniques to provide snow depth on fast ice in the coastal Antarctic. The snow distribution from SnowModel accurately captures the measured distribution in November 2011 and produces a swe mean value that is 0.02 m above the mean of *in situ* validation, but when sea ice is segmented by fastening date large deviations of up to 0.05 m are present in the east where the model has overestimated snow depth. This accurately captures the mechanism of snowfall and transport driven by the topography of Ross Island, but the rates are higher than in reality. ERA-Interim swe is 0.01 m lower than *in situ* measurements but its coarse resolution prevented the adjustment of precipitation to sea ice fastening dates. AMSR-E snow depth information suffers from problems already documented in the literature, and we postulate here that its performance may have again been influenced by rough sea ice. In this investigation the snow distribution produced by AMSR-E was opposite to that provided by SnowModel and measured *in situ*. The uncertainty in the snow depth estimates manifest themselves in the sea ice thickness estimates from CS-2. A large range in thickness of over 2 m is expected if the actual surface the freeboard represents remains ambiguous. Here we find CS-2 freeboard measurements are most likely representative of a mean scattering horizon between 0.05-0.10 m beneath the air-snow interface. It is impossible to confidentially constrain this number without reducing uncertainty in the established sea surface height from which the freeboard is estimated. An improved understanding of the CS-2 freeboard measurement will be critical to accurately provide sea ice thickness estimates over varying snow and sea ice conditions in the Southern Ocean.

Modelled snow information has the potential to produce a time series of snow depth on sea ice. Here we show that with improvements to redistribution mechanisms and adequate representation of the effect of topographic features atmospheric models are capable of producing snow depths at least as reliable as contemporary passive microwave algorithms. Future work must begin to assess the usefulness of SnowModel products over the larger pack ice areas, and critically develop a method to (1) incorporate sea ice drift through the atmospheric model domains, and (2) account for snow loss to leads.

8 Acknowledgments

Gratitude is shown for the support of Antarctica New Zealand and Scott Base staff during the 2011/12 Antarctic field season permitting the collection of *in situ* snow and sea ice measurements, and the members of field team K053. We thank Ethan Dale for compiling and providing ERA-Interim data. Thanks is given to Oliver Marsh and Christian Wild for productive discussions about the topic. This work was partially supported by NIWA subcontract C01X1226 (Ross Sea Climate and Ecosystem) and the Marsden Fund Council from Government funding, managed by Royal Society Te Apārangi. We are grateful to Victoria Landgraf, Troy Beaumont, and Grant Cottle from Antarctica New Zealand's Scott Base 2011 winter-over team for making the July sea ice thickness measurements as part of the winter support of a University of Otago Research Grant funded project (PI: Pat Langhorne, AI: Inga Smith). We thank Peter Green and Inga Smith for their insights into the 2011 sea ice growth rates, which were supported by the fieldwork and analytical efforts of Greg Leonard, Alex Gough, Tim Haskell, Pat Langhorne, Jonothan Everts, and by the technical advice of Joe Trodahl and Daniel Pringle, and the technical support of Myles Thayer, Peter Stroud and Richard Sparrow. This research was completed at Gateway Antarctica, University of Canterbury, Christchurch, New Zealand.

The Cryosphere Discuss., https://doi.org/10.5194/tc-2018-92
Manuscript under review for journal The Cryosphere
Discussion started: 28 May 2018

9 References

Agustsson, H & Olafsson, H. 2007. Simulating a severe windstorm in complex terrain. Meteorol Atmos Phys, 103, 173–185, doi: 10.1007/s00703-008-0347-y.

Beaven, S. G., Lockhart, G. L., Gogineni, S. P., Hossetnmostafa, A. R., Jezek, K., Gow, A. J., Perovich, D. K., Fung, A. K. & Tjuatja, S. 1995. Laboratory measurements of radar backscatter from bare and snow-covered saline ice sheets. International Journal of Remote Sensing, 16, 851-876.

Bouffard, J. 2015. CryoSat-2 Level 2 product evolutions and quality improvements in Baseline C. Available at: https://earth.esa.int/documents/10174/1773005/C2-Evolution-BaselineC-Level2-V3.

Bromwich, D.H., Hines K.M & Bai, L.S. 2009. Development and testing of Polar WRF: 2. Arctic Ocean. J. Geophys. Res, 114, D08122, doi: 10.1029/2008JD010300.

Bromwich, D. H. & Fogt, R. L. 2004. Strong Trends in the Skill of the ERA-40 and NCEP–NCAR Reanalyses in the High and Midlatitudes of the Southern Hemisphere, 1958–2001. Journal of Climate, 17, 4603-4619, doi: 10.1175/3241.1.

Chen, F. & Dudhia, J. 2001. Coupling an Advanced Land Surface–Hydrology Model with the Penn State–NCAR MM5 Modeling System. Part I: Model Implementation and Sensitivity. Monthly Weather Review, 129, 569-585, doi: 10.1175/1520-0493(2001)129<0569:CAALSH>2.0.CO;2.

Comiso, C., Cavalieri, J. & Markus, T. 2003. Sea Ice Concentration, Ice Temperature, and Snow Depth Using AMSR-E Data. IEEE Transactions on Geoscience and Remote Sensing, 41, 243-252, doi: 10.1109/TGRS.2002.808317.

Dee, D. P., Uppala, S. M., Simmons, A. J., Berrisford, P., Poli, P., Kobayashi, S., Andrae, U., Balmaseda, M. A., Balsamo, G., Bauer, P., Bechtold, P., Beljaars, A. C. M., van de Berg, L., Bidlot, J., Bormann, N., Delsol, C., Dragani, R., Fuentes, M., Geer, A. J., Haimberger, L., Healy, S. B., Hersbach, H., Hólm, E. V., Isaksen, L., Kållberg, P., Köhler, M., Matricardi, M., Mcnally, A. P., Monge-Sanz, B. M., Morcrette, J. J., Park, B. K., Peubey, C., De Rosnay, P., Tavolato, C., Thépaut, J. N. & Vitart, F. 2011. The ERA-Interim reanalysis: configuration and performance of the data assimilation system. Quarterly Journal of the Royal Meteorological Society, 137, 553-597, doi: 10.1002/qj.828.

Dudhia, J. 1989. Numerical study of convection observed during the winter monsoon experiment using a mesoscale two-dimensional model. Journal of Atmospheric Sciences, 46, 3077-3107, doi: 10.1175/1520-0469(1989)046<3077:NSOCOD>2.0.CO;2.

Fichefet, T. & Maqueda, M. A. M. 1999. Modelling the influence of snow accumulation and snow-ice formation on the seasonal cycle of the Antarctic sea-ice cover. Climate Dynamics, 15, 251-268, doi: 10.1007/s003820050280.

Frazer, E. K., Langhorne, P. J., Williams, M. J. M., Goetz, K. T. & Costa, D. P. Under review. A method for correcting seal-borne oceanographic data and application to the estimation of regional sea ice thickness. Journal of Marine Systems.

Giles, K. A., Laxon, S. W. & Worby, A. P. 2008. Antarctic sea ice elevation from satellite radar altimetry. Geophysical Research Letters, 35, L03503, doi: 10.1029/2007GL031572.

Gough, A. J., Mahoney, A. R., Langhorne, P. J., Williams, M. J. M. & Haskell, T. G. 2012. Sea ice salinity and structure: A winter time series of salinity and its distribution. Journal of Geophysical Research: Oceans, 117, C03008, doi:10.1029/2011JC007527.

Hallikainen, M., Ulaby, F. & Abdelrazik, M. 1986. Dielectric properties of snow in the 3 to 37 GHz range. IEEE Transactions on Antennas and Propagation, 34, 1329-1340.

Hines, K. M., Bromwich, D. H., Bai, L., Bitz, C. M., Powers, J. G. & Manning, K. W. 2015. Sea Ice Enhancements to Polar WRF. Monthly Weather Review, 143, 2363-2385, doi: 10.1175/MWR-D-14-00344.1.

Hong, S.-Y. & Lim, J.-O. J. 2006. The WRF Single-Moment 6-Class Microphysics Scheme (WSM6). Journal of the Korean Meteorological Society, 42, 129-151.

Kaleschke, L., Tian-kunze, X., Maaß, N., Mäkynen, M. & Drusch, M. 2012. Sea ice thickness retrieval from SMOS brightness temperatures during the Arctic freeze-up period. Geophysical Research Letters, 39, L05501, doi: 10.1029/2012GL050916.

Kern, S. & Ozsoy-Çiçek, B. 2016. Satellite Remote Sensing of Snow Depth on Antarctic Sea Ice: An Inter-Comparison of Two Empirical Approaches. Remote Sensing, 8(6), 450, doi: 10.3390/rs8060450.

Kern, S., Ozsoy-Çiçek, B., Willmes, S., Nicolaus, M., Haas, C. & Ackley, S. 2011. An intercomparison between AMSR-E snow-depth and satellite C- and Ku-band radar backscatter data for Antarctic sea ice. Annals of Glaciology, 52(57), 279-290. doi:10.3189/172756411795931750.

Kurtz, N. T., Galin, N. & Studinger, M. 2014. An improved CryoSat-2 sea ice freeboard retrieval algorithm through the use of waveform fitting. The Cryosphere, 8, 1217-1237, https://doi.org/10.5194/tc-8-1217-2014.

Kurtz, N. T. & Markus, T. 2012. Satellite observations of Antarctic sea ice thickness and volume. Journal of Geophysical Research: Oceans, 117, C08025, doi: 10.1029/2012JC008141.

Kwok, R. 2014. Simulated effects of a snow layer on retrieval of CryoSat-2 sea ice freeboard. Geophysical Research Letters, 41, 5014–5020, doi: 10.1002/2014GL060993.

Kwok, R. & Cunningham, G. F. 2008. ICESat over Arctic sea ice: Estimation of snow depth and ice thickness. Journal of Geophysical Research: Oceans, 113, C08010, doi: 10.1029/2008JC004753.

Kwok, R., Nghiem, S. V., Yueh, S. H. & Huynh, D. D. 1995. Retrieval of thin ice thickness from multifrequency polarimetric SAR data. Remote Sensing of Environment, 51, 361-374, doi: 10.1016/0034-4257(94)00017-H.

Laxon, S., Peacock, N. & Smith, D. 2003. High interannual variability of sea ice thickness in the Arctic region. Nature, 425, 947-950, doi: 10.1038/nature02050.

Laxon, S. W., Giles, K. A., Ridout, A. L., Wingham, D. J., Willatt, R., Cullen, R., Kwok, R., Schweiger, A., Zhang, J., Haas, C., Hendricks, S., Krishfield, R., Kurtz, N., Farrell, S. &

Davidson, M. 2013. CryoSat-2 estimates of Arctic sea ice thickness and volume. Geophysical Research Letters, 40, 732-737, doi: 10.1002/grl.50193.

Leonard, K. C. & Maksym, T. 2011. The importance of wind-blown snow redistribution to snow accumulation on Bellingshausen Sea ice. Annals of Glaciology, 52, 271-278, doi: 10.3189/172756411795931651.

Liston, G. E., Polashenski, C. , Rösel, A. , Itkin, P. , King, J. , Merkouriadi, I. and Haapala, J. 2018. A Distributed Snow Evolution Model for Sea Ice Applications (SnowModel). J. Geophys. Res. Oceans. Accepted Author Manuscript. . doi:10.1002/2017JC013706.

Liston, G. E. & Hiemstra, C. A. 2011. Representing Grass– and Shrub–Snow–Atmosphere Interactions in Climate System Models. Journal of Climate, 24, 2061-2079, doi: 10.1175/2010JCLI4028.1.

Liston, G. E. & Hiemstra, C. A. 2008. A Simple Data Assimilation System for Complex Snow Distributions (SnowAssim). Journal of Hydrometeorology, 9, 989-1004, doi: https://doi.org/10.1175/2008JHM871.1.

Liston, G. E., Haehnel, R. B., Sturm, M., Hiemstra, C. A., Berezovskaya, S. & Tabler, R. D. 2007. Instruments and Methods Simulating complex snow distributions in windy environments using SnowTran-3D. Journal of Glaciology, 53, 241-256, doi: https://doi.org/10.3189/172756507782202865.

Liston, G. E. & Elder, K. 2006a. A Distributed Snow-Evolution Modeling System (SnowModel). Journal of Hydrometeorology, 7, 1259-1276, doi: 10.1175/JHM548.1.

Liston, G. E. & Elder, K. 2006b. A Meteorological Distribution System for High-Resolution Terrestrial Modeling (MicroMet). Journal of Hydrometeorology, 7, 217-234, doi: 10.1175/JHM486.1.

Liston, G. E. & Winther, J.-G. 2005. Antarctic Surface and Subsurface Snow and Ice Melt Fluxes. Journal of Climate, 18, 1469-1481, doi: 10.1175/JCLI3344.1.

Liston, G. E., Pielke, R. A. & Greene, E. M. 1999. Improving first-order snow-related deficiencies in a regional climate model. Journal of Geophysical Research: Atmospheres, 104, 19559-19567, doi: 10.1029/1999JD900055.

Liston, G. E. & Sturm, M. 1998. A snow-transport model for complex terrain. Journal of Glaciology, 44, 498-516, doi: 10.3189/S0022143000002021.

Maksym, T. & Markus, T. 2008. Antarctic sea ice thickness and snow-to-ice conversion from atmospheric reanalysis and passive microwave snow depth. Journal of Geophysical Research: Oceans, 113, C02S12, doi:10.1029/2006JC004085.

Markus, T. & Cavalieri, D. J. 1998. Snow Depth Distribution Over Sea Ice in the Southern Ocean from Satellite Passive Microwave Data. Antarctic Sea Ice: Physical Processes, Interactions and Variability. American Geophysical Union. M. O. Jeffries (Ed.). doi:10.1029/AR074p0019.

The Cryosphere Discuss., https://doi.org/10.5194/tc-2018-92
Manuscript under review for journal The Cryosphere
Discussion started: 28 May 2018

The Cryosphere Discussions

Markus, T. & Cavalieri, D. J. 2006. Interannual and regional variability of Southern Ocean snow on sea ice. Annals of Glaciology, 44, 53-57, doi: 10.3189/172756406781811475.

Massom, R. A., Eicken, H., Hass, C., Jeffries, M. O., Drinkwater, M. R., Sturm, M., Worby, A. P., Wu, X., Lytle, V. I., Ushio, S., Morris, K., Reid, P. A., Warren, S. G. & Allison, I. 2001. Snow on Antarctic sea ice. Reviews of Geophysics, 39(3), 413–445, doi:10.1029/2000RG000085.

Maykut, G. & Untersteiner, N. 1971. Some results from a time dependent thermodynamic model of sea ice. J. Geophys. Res, 76, 1550-1575.

Mernild, S.H., Liston, G.E., Hasholt, B & Knudsen, N.T. 2006. Snow distribution and melt modeling for Mittivakkat Glacier, Ammassalik Island, southeast Greenland. J. Hydrometeorology, 7, 808-824, doi: 10.1175/JHM522.1.

Mlawer, E. J., Taubman, S. J., Brown, P. D., Iacono, M. J. & Clough, S. A. 1997. Radiative transfer for inhomogeneous atmospheres: RRTM, a validated correlated-k model for the longwave. Journal of Geophysical Research: Atmospheres, 102, 16663-16682.

Nakanishi, M. 2001. Improvement of the Mellor-Yamada turbulence closure model based on large-eddy simulation data. Boundary Layer Meteorology, 99, 349-378, doi: 10.1023/A:1018915827400.

Nakanishi, M. & Niino, H. 2004. An Improved Mellor–Yamada Level-3 Model with Condensation Physics: Its Design and Verification. Boundary-Layer Meteorology, 112, 1-31, doi:10.1023/B:BOUN.0000020164.04146.98.

Nakanishi, M. & Niino, H. 2006. An Improved Mellor–Yamada Level-3 Model: Its Numerical Stability and Application to a Regional Prediction of Advection Fog. Boundary-Layer Meteorology, 119, 397-407, doi: 10.1007/s10546-005-9030-8.

Nicolas, J. P. & Bromwich, D. H. 2011. Precipitation Changes in High Southern Latitudes from Global Reanalyses: A Cautionary Tale. Surveys in Geophysics, 32, 475-494, doi: 10.1007/s10712-011-9114-6.

Olafsson, H & Agustsson H. 2009. Gravity wave breaking in easterly flow over Greenland and associated low level barrier-and reverse tip-jets. Meteorol. Atmos. Phys, 104, 191-197, doi: 10.1007/s00703-009-0024-9.

Pope, A., Wagner, P., Johnson, R., Shutler, J. D., Baeseman, J. & Newman, L. 2016. Community review of Southern Ocean satellite data needs. Antarctic Science, 29, 97-138, doi: 10.1017/S0954102016000390.

Price, D., Beckers, J., Ricker, R., Kurtz, N., Rack, W., Haas, C., Helm, V., Hendricks, S., Leonard, G. & Langhorne, P. J. 2015. Evaluation of CryoSat-2 derived sea-ice freeboard over fast ice in McMurdo Sound, Antarctica. Journal of Glaciology, 61, 285-300, doi: 10.3189/2015JoG14J157.

Price, D., Rack, W., Langhorne, P. J., Haas, C., Leonard, G. & Barnsdale, K. 2014. The sub-ice platelet layer and its influence on freeboard to thickness conversion of Antarctic sea ice. The Cryosphere, 8, 1031-1039, doi: 10.5194/tc-8-1031-2014.

Purdie, C. R., Langhorne, P. J., Leonard, G. H. & Haskell, T. G. 2006. Growth of first-year landfast Antarctic sea ice determined from winter temperature measurements. Annals of Glaciology, 44, 170-176, doi: 10.3189/172756406781811853.

Ricker, R., Hendricks, S., Helm, V., Skourup, H. & Davidson, M. 2014. Sensitivity of CryoSat-2 Arctic sea-ice freeboard and thickness on radar-waveform interpretation. The Cryosphere, 8, 1607-1622, doi: 10.5194/tc-8-1607-2014.

Ricker, R., Hendricks, S., Kaleschke, L., Tian-Kunze, X., King, J. & Haas, C. 2017. A weekly Arctic sea-ice thickness data record from merged CryoSat-2 and SMOS satellite data. The Cryosphere, 11, 1607-1623, doi: 10.5194/tc-11-1607-2017.

Schwegmann, S., Rinne, E., Ricker, R., Hendricks, S. & Helm, V. 2016. About the consistency between Envisat and CryoSat-2 radar freeboard retrieval over Antarctic sea ice. The Cryosphere, 10, 1415-1425, doi: 10.5194/tc-10-1415-2016.

Skamarock, W. C., Klemp, J. B., Dudhia, J., Gill, D. O., Barker, D. M., Duda, M. G., Huang, X.-Y., Wang, W. & Powers, J. G. 2008. A Description of the Advanced Research WRF Version 3. NCAR Technical Note.

Stroeve, J. C., Markus, T., Maslanik, J. A., Cavalieri, D. J., Gasiewski, A. J., Heinrichs, J. F., Holmgren, J., Perovich, D. K. & Sturm, M. 2006. Impact of Surface Roughness on AMSR-E Sea Ice Products. IEEE Transactions on Geoscience and Remote Sensing, 44, 3103-3117, doi: 10.1109/TGRS.2006.880619.

Warren, S. G., Rigor, I. G., Untersteiner, N., Radionov, V. F., Bryazgin, N. N., Aleksandrov, Y. I. & Colony, R. 1999. Snow Depth on Arctic Sea Ice. Journal of Climate, 12, 1814-1829, doi: 10.1175/1520-0442(1999)012<1814:SDOASI>2.0.CO;2.

Willatt, R. C., Giles, K. A., Laxon, S. W., Stone-Drake, L. & Worby, A. P. 2010. Field Investigations of Ku-Band Radar Penetration Into Snow Cover on Antarctic Sea Ice. IEEE Transactions on Geoscience and Remote Sensing, 48, 365-372, doi: 10.1109/TGRS.2009.2028237.

Wingham, D. J., Francis, C. R., Baker, S., Bouzinac, C., Brockley, D., Cullen, R., De Chateau-Thierry, P., Laxon, S. W., Mallow, U., Mavrocordatos, C., Phalippou, L., Ratier, G., Rey, L., Rostan, F., Viau, P. & Wallis, D. W. 2006. CryoSat: A mission to determine the fluctuations in Earth's land and marine ice fields. Advances in Space Research, 37, 841-871, doi: 10.1016/j.asr.2005.07.027.

Worby, A. P., Geiger, C. A., Paget, M. J., Woert, M. L. V., Ackley, S. F. & DeLiberty, T. L. 2008a. Thickness distribution of Antarctic sea ice. Journal of Geophysical Research: Oceans, 113, C05S92, doi: 10.1029/2007JC004254.

Worby, A. P., Markus, T., Steer, A. D., Lytle, V. I. & Massom, R. A. 2008b. Evaluation of AMSR-E snow depth product over East Antarctic sea ice using in situ measurements and aerial photography. Journal of Geophysical Research: Oceans, 113, C05S94, doi: 10.1029/2007JC004181.

Wu, X., Budd, W. F., Lytle, V. I. & Massom, R. A. 1999. The effect of snow on Antarctic sea ice simulations in a coupled atmosphere-sea ice model. Climate Dynamics, 15, 127-143, doi: 10.1007/s003820050272.